



The fast formation of full Cu_3Sn solder joints in Cu/Sn/Cu system by thermal gradient bonding

Zuozhu Yin¹ · Fenglian Sun² · Mengjiao Guo²

Received: 15 September 2018 / Accepted: 29 November 2018 / Published online: 3 December 2018
© Springer Science+Business Media, LLC, part of Springer Nature 2018

Abstract

To form full intermetallic compounds (IMCs) solder joints becomes widely available for the die bonding of the third generation semiconductor power devices. The fast formation of Cu_3Sn in Cu/Sn(10 μm)/Cu solder joints were investigated by thermal compression bonding in a few seconds and under a low pressure of 0.1 MPa at ambient temperature. The results show that the temperature gradient produced by thermal compression bonding contributes to enhancing the interfacial reaction at the liquid Sn/solid Cu metallization interface. The scallop-liked Cu_6Sn_5 is formed while planar-liked Cu_3Sn is formed between Cu and Cu_6Sn_5 at initial bonding stage. After that, the growth rate of scallop-liked Cu_6Sn_5 layer from cold end is faster than that from hot end and the thin planar-liked Cu_3Sn layer becomes thick. This abnormal growth behavior of Cu_6Sn_5 is due to the fact that Cu atoms migrate from hot end to cold end by temperature gradient. The middle Sn layer is completely consumed with increasing bonding time. Cu_6Sn_5 and Cu_3Sn are consisted of the solder joints and the planar-liked Cu_3Sn grows with a transition to scallop-liked morphology until the full Cu_3Sn solder joint is eventually formed, which indicates that the formation time of full IMCs solder joints can be narrowed by temperature gradient. This bonding process provides a new solution for the rapid acquisition of interconnect material for the third generation semiconductor power devices.

1 Introduction

Compared to conventional Si semiconductors, the third generation semiconductors (such as SiC and GaN) have emerged as potential substitute productions, due to their outstanding advantages, such as wide band-gap, high thermal conductivity, high electron drift velocity, which are designed as a driver for power devices working in harsh environment (–100 to 600 °C) [1–3]. The stresses caused by interconnect materials and chips are particularly prominent during high service temperature for the power device. Therefore, it is very crucial to investigate the interconnect material used for the third generation semiconductor power devices. The interconnect material needs meet the following aspects: (1) It can service in high temperature; (2) It can react with other metals in a relative low temperature; (3) It has better

thermal conductivity, electrical conductivity and mechanical property.

Compared to Sn-based solder alloys [4, 5], traditional Pb-based solder alloys can service in high temperature, but they are explicitly banned by the Restriction of Hazardous Substances (RoHS) requirements for their application in electronic packaging field [6, 7]. Other high melting temperature lead-free solder alloys, such as Au–Sn solder alloy, Bi-based solder alloy, Zn-based solder alloy. The melting temperature of Au–Sn solder alloy is 280 °C, but its high cost makes it not appropriate for large area in die attachments [8, 9]. The melting temperature of Bi-based solder alloy is 263 °C, but its brittleness is a big drawback for its wide application [10]. The melting temperature of Zn-based solder alloy is 320 °C, but its poor oxidation resistance is a big problem [11].

Recently, this difficult problem has been proven to be solved by nano Ag sintering process [12–15] and transient liquid phase process (TLP) [16, 17]. Nano-Ag sintering is a promising packaging method for high temperature service, which has a good electrical conductivity and increaseable melting point. However, nano-Ag sintering has its drawbacks for low resistance to electro-migration and easy to oxidation. Therefore, TLP bonding technology is the most promising technology for the third generation

✉ Zuozhu Yin
yinzuo@163.com

¹ Department of Engineering, Harbin University, 109# Zhongxin Street, Harbin 150086, People's Republic of China

² School of Materials Science and Engineering, Harbin University of Science and Technology, Harbin 150040, People's Republic of China

semiconductor power devices [18–20]. The principle of TLP bonding technology is that a low melting temperature metal (Sn, In) melts to react with high melting temperature metal (Cu, Ag, Au) to form high melting temperature intermetallic compounds (IMCs). However, the formation process of full IMCs solder joint needs very long time (> 100 min). Therefore, it is a key point to form full IMCs solder joints rapidly and efficiently for the interconnect material for the next generation semiconductor power devices.

Recently, researchers have used different TLP methods to form full IMCs solder joints rapidly and efficiently. A full Cu_3Sn -based solder joint is fabricated by micro resistance spot welding in a few 100 ms [21]. A full Cu_3Sn solder joint is obtained by induction heating process in a few minutes [22]. A full Ni_3Sn_4 solder joint is fabricated by ultrasonic assisted soldering process in a few seconds [23], but the cost is very expensive and it is very hard to operate it, which make it hard to be considered for large area application. The thermal compression device is cheap and easy to operate, the temperature is very convenient to be controlled. Furthermore, a stable and reliable solder joint can be obtained [24]. The principle of the thermal compression bonding is that the heat resistance generated by the resistance wire is transmitted to the interconnect material by heat transfer. Therefore, the temperature gradient is generated across the interconnect material. Due to the thin interconnect material layer, the phenomenon caused by temperature gradient becomes obvious.

This paper is focused on the fast formation of full Cu_3Sn solder joint in Cu/Sn/Cu system by thermal compression bonding. Microstructure evolution and phase transformation of the Cu/Sn/Cu system during TLP bonding under the temperature gradient are investigated. A new idea (temperature gradient bonding) is proposed for fabricating full IMC solder joint rapidly and efficiently.

2 Experimental section

Experimental setup of thermal compression bonding process and schematic illustration of the Cu/Sn/Cu sandwich structure interconnection system are represented in Fig. 1. The thickness of interlayer pure Sn foil (99.9% purity) is 10 μm and the thickness of pure Cu substrate is 100 μm . One side of the Cu substrate is polished and then the polished side is fixed, after that, the pure Sn layer was placed between two pieces of Cu substrate. Before soldering, the sides of the Cu substrates were washed by HCl so as to remove the surface oxide products, and then placed in hot air to dry. The Cu/Sn/Cu sandwich structure is connected by thermo compression bonding machine (JUKE-H1200D, China). After bonding process, the samples were cooled to room temperature in the air. The temperature is controlled by power controller. The temperature is set at 400 $^\circ\text{C}$ by the power controller, which means that the temperature of hot end is 400 $^\circ\text{C}$. The bonding pressure was 0.016 MPa during the bonding process. According to the schematic of the thermal compression bonding, the bottom interface is the cold end while the top interface is the hot end. The profile of the bonding process during thermal compression bonding is shown in Fig. 2. In the study, bonding time is the high temperature holding time.

In order to observe the microstructure evolution of interfacial IMC at the molten Sn/solid Cu metallization interface, the cross-sectional Cu/IMC/Sn/IMC/Cu solder joints are deeply etched with 10 mL vol% HF + 10 mL vol% HNO_3 + 20 mL $\text{C}_2\text{H}_5\text{OH}$ so as to remove the unreacted Sn solder. The cross-sectional microstructure evolution of the Cu/IMC/Sn/IMC/Cu solder joints are characterized by optical microscope (OM) and scanning electron microscope (SEM). The interfacial element is analyzed by EDS. The IMC layer thickness is measured by Photoshop CS6 software. The average thickness of interfacial IMC layer is obtained through dividing the total area of the IMC layer by the length of the observation area. In order to

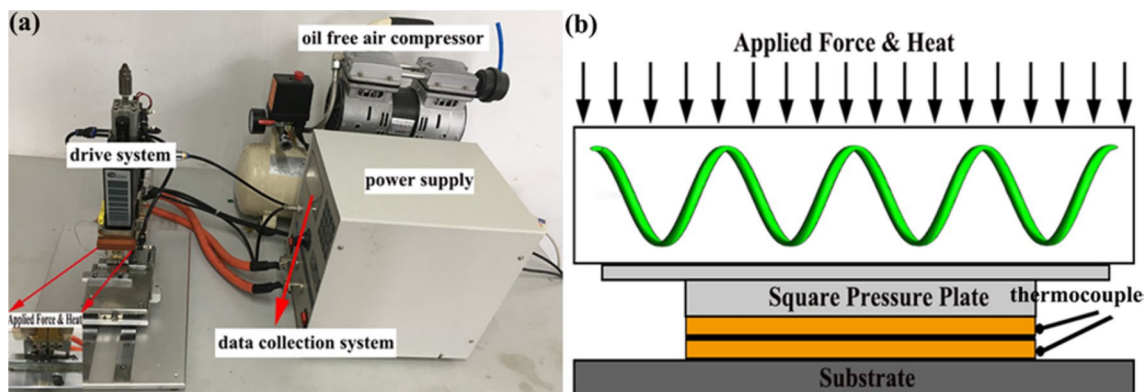


Fig. 1 a Experimental setup of thermal compression bonding process and b schematic illustration of the Cu/Sn/Cu sandwich structure interconnection system

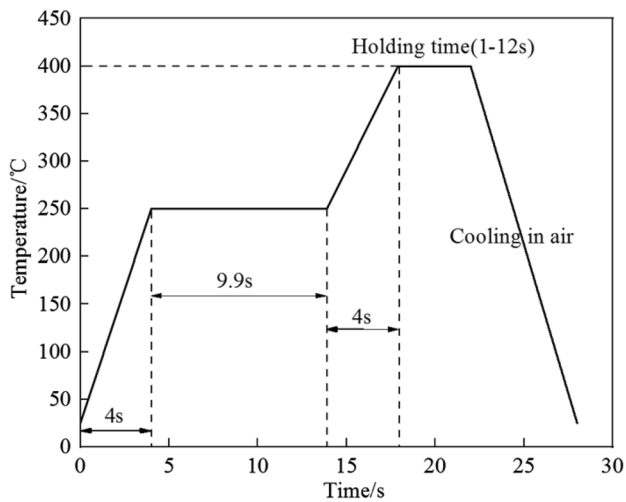


Fig. 2 Profile of the bonding process during thermal compression bonding

make the measured data more accurate, every sample is measured at least five times.

3 Results

3.1 Simulated temperature distribution of Cu/Sn/Cu sandwich structure

In order to understand the temperature distribution of liquid solder alloy layer, the temperature distribution of liquid solder was simulated by FEM. In order to simplify it, the 2D model was established by ANSYS 15.0 software and only the heat transfer and heat convection are considered. In order to estimate the temperature gradient across the solder layer, the temperature gradient of Cu/Sn/Cu sandwich structure is simulated. During thermal compression bonding process, air convection and heat radiation are the main ways of heat transfer, this is due to the fact that the Cu has a high thermal conductivity ($401 \text{ W m}^{-1} \text{ K}^{-1}$). The equation for the rate of convective heat transfer can be expressed as:

$$q = h_c \Delta T \quad (1)$$

where q is the rate of convective heat transfer, ΔT is the temperature difference between surface and liquid, h_c is the convective heat transfer coefficient. The surface of the interconnect material is an ideal blackbody surrounded with gray surface. The radiative heat transfer coefficient h_r can be expressed as:

$$h_r = \varepsilon \sigma (T_s - T_r) (T_s^2 + T_r^2) \quad (2)$$

where ε is emissivity, σ is the Boltzmann constant, T_s and T_r are the surface temperature of the connection material and the room temperature, respectively. The combined heat

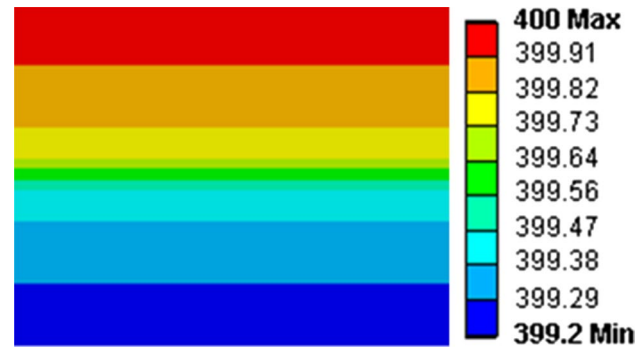


Fig. 3 Simulated temperature distribution across the solder layer by thermal migration

transfer coefficient (h_t) of convection and radiation can be written as:

$$h_t = h_c + h_r \quad (3)$$

Figure 3 shows the simulated temperature distribution across the liquid solder layer during temperature gradient bonding using FEM. The simulated temperature can be measured by FEM according to the solder layer thickness. Because of the hot end of the temperature is controlled by power controller, when the temperature is set at $400 \text{ }^\circ\text{C}$ by the power controller, which means that the temperature of hot end is $400 \text{ }^\circ\text{C}$, therefore the hot end of the simulated temperature is $400 \text{ }^\circ\text{C}$, the cold end of the simulated temperature is $399.2 \text{ }^\circ\text{C}$. The FEM result shows that the change of temperature between hot end and cold end is $0.8 \text{ }^\circ\text{C}$. Although the change of temperature is very small, the temperature gradient across liquid solder alloy is over $800 \text{ }^\circ\text{C/cm}$. As is reported in the literature [25], when the temperature gradient is over $400 \text{ }^\circ\text{C/cm}$, The activated Cu atoms can across the liquid Sn layer through thermal migration. Therefore, Cu atoms are moved from hot end to cold end by the temperature gradient of $800 \text{ }^\circ\text{C/cm}$.

3.2 The interfacial microstructure evolution of Cu/Sn/Cu sandwich structure

Figure 4 shows the interfacial microstructure evolution of Cu/Sn/Cu sandwich structure. The end which closes to the heat source is hot end, the other is cold end. The morphology of Cu_6Sn_5 shows scallop-like shape. When the bonding time up to 1 s, the Cu_6Sn_5 layer in hot end and cold end show symmetry growth, as is shown in Fig. 4a. Big Cu_6Sn_5 grains in cold end begin to grow towards to small Cu_6Sn_5 grains in hot cold with increasing bonding time. The growth rate of Cu_6Sn_5 in cold end is faster than that of in hot end. In order to identify the phase constitution of the Cu/Sn/Cu interface, the interfacial reaction of the Cu/Sn/Cu system is investigated by SEM. The temperature of cold end is not

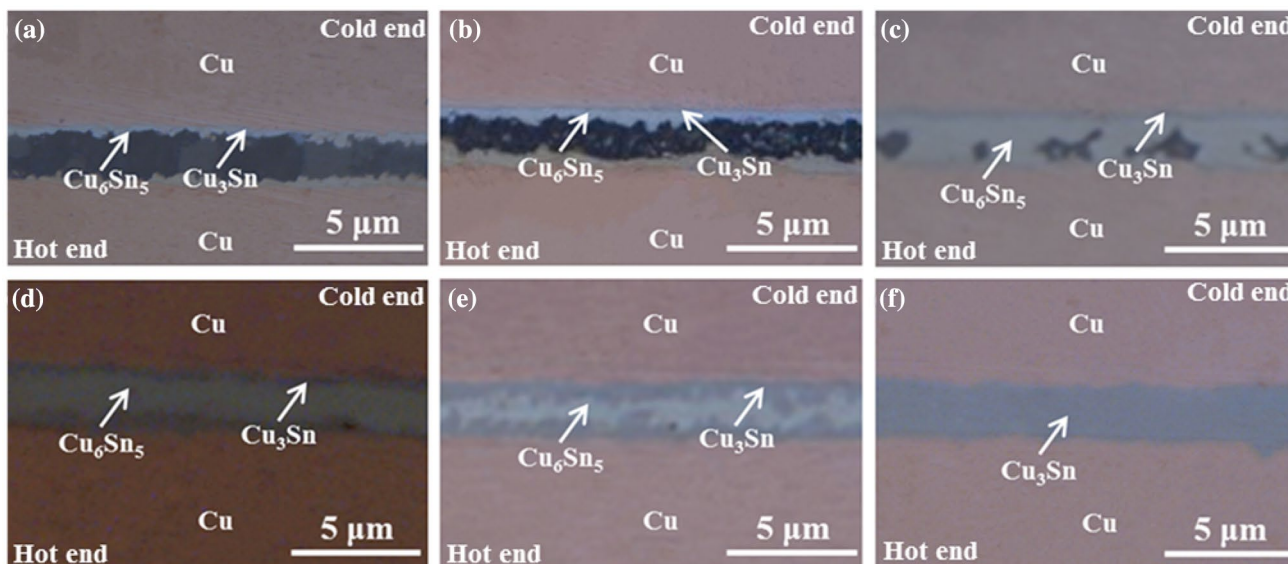


Fig. 4 The interfacial microstructure evolution of Cu/Sn/Cu sandwich structure at different bonding time: **a** 1 s; **b** 3 s; **c** 6 s; **d** 7 s; **e** 8 s; **f** 9.9 s

measured directly, but the hot end is measured directly. The simulated temperature can be measured by FEM according to the solder layer thickness. Because of the hot end of the temperature is controlled by power controller, when the temperature is set at 400 °C by the power controller, which means that the temperature of hot end is 400 °C, therefore, the hot end of the simulated temperature is 400 °C, the cold end of the simulated temperature is 399.2 °C. Moreover, the references [25–28] are introduced that the temperature gradient will contribute to the abnormal of interfacial IMC layer growth. Although the temperature is not measured directly, the abnormal growth of interfacial IMC can be seen in Fig. 4, which means that the solder layer will form temperature gradient. Figure 5 presents Cu/Sn/Cu interfacial microstructure at bonding time of 9.9 s and corresponding

EDS line scan profiles by thermal compression bonding. The interfacial IMC layer is characterized by 75.1% Cu, 24.9% Sn, supposed to be Cu₃Sn. Nearly all measured data of Cu atoms exceeded their limiting solubility in Sn (0.28 wt%) and the super-saturation of Cu atoms near the cold end is significantly higher than that of near the hot end, which indicate that Cu atoms diffuse and deposit along the temperature gradient direction.

The schematic diagram of interfacial microstructure evolution of Cu/Sn/Cu solder joint by temperature gradient bonding is shown in Fig. 6. At initial bonding time, the temperature gradient across the liquid Sn layer is not apparent, therefore, the interfacial IMCs show symmetry growth. With the increasing bonding time, the equilibrium of Cu atom solubility from hot end is broken, and

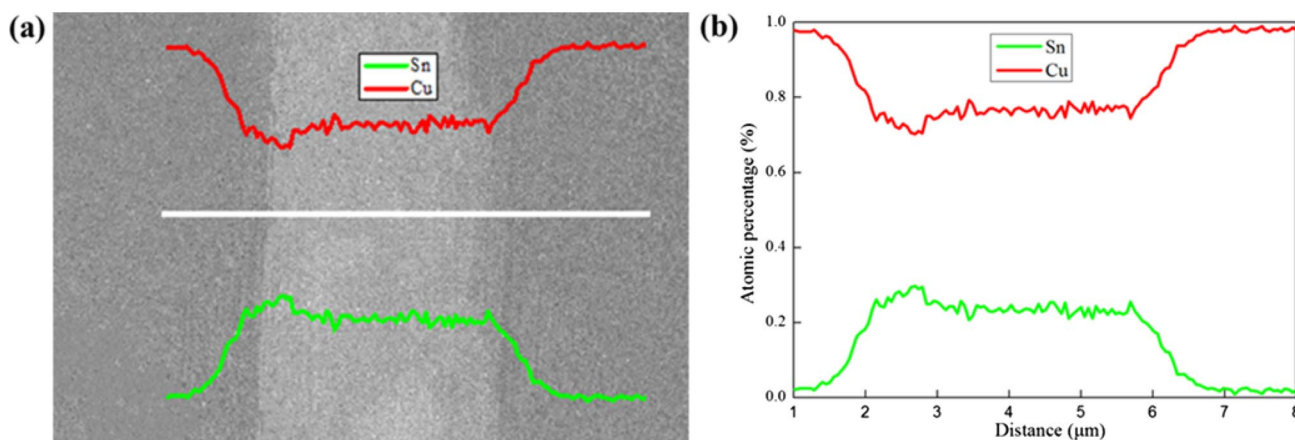


Fig. 5 Interfacial microstructure **a** and EDS line scan profiles **b** of bonding time at 9.9 s by thermal compression bonding

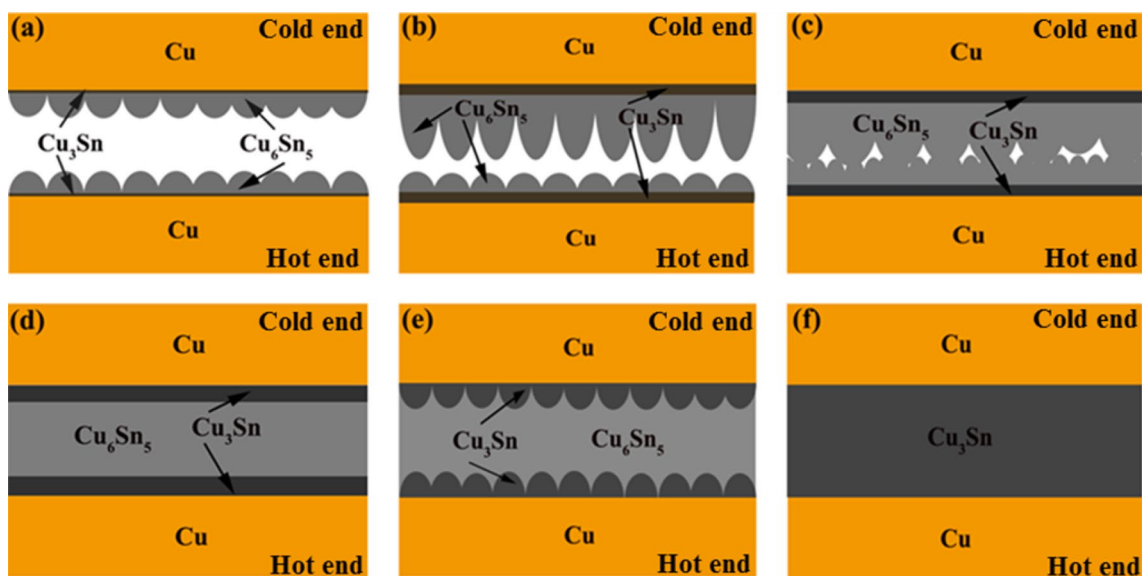


Fig. 6 The schematic of interfacial microstructure evolution of Cu/Sn/Cu solder joint by temperature gradient bonding

the newly dissolved Cu atoms migrate from hot end to cold end under the temperature gradient. At the same time, the concentration of Cu atoms in molten Sn solder from hot end will drop below the equilibrium solubility. In order to maintain this solute balance, the dissolution of Cu_6Sn_5 from hot end will be promoted to replenish the Cu solute in the molten Sn. The dissolved Cu atoms from hot end are continuously migrated to the cold end under temperature gradient, causing the Cu solute concentration from cold end to increase rapidly. When the solute concentration reaches a certain level, the Cu_6Sn_5 begins to precipitate, which promotes the growth of Cu_6Sn_5 from cold end. The Cu_6Sn_5 grains from hot end and cold end begin to asymmetry growth, which makes the Cu_6Sn_5 grains from cold end become big, as is shown in Fig. 6c. The growth rate of large Cu_6Sn_5 grain in cold end is faster than that of small Cu_6Sn_5 grain in hot end. The Cu_6Sn_5 grains are fused into single grain and the middle molten Sn layer is separated into “Sn islands”. When all “Sn islands” are consumed, the interface IMCs are consisted of Cu_6Sn_5 and Cu_3Sn , as is shown in Fig. 6d. After then, the main chemical reaction is that Cu_6Sn_5 and Cu react with each other to form Cu_3Sn , planar-liked Cu_3Sn layer will change to scallop-liked Cu_3Sn layer, as is shown in Fig. 6e, at same time, the solder joints that is consisted of full IMCs no longer exist the migration of Cu atom. As the time continues to increase, Cu_6Sn_5 continues to be consumed until all Cu_6Sn_5 layer transform into Cu_3Sn layer, eventually forming a full Cu_3Sn solder joints, as is shown in Fig. 6f.

3.3 Growth kinetics of interfacial IMC

In order to understand the effect of temperature gradient on the interfacial IMC growth, the interfacial IMC growth kinetics can be expressed with the empirical power law as follows:

$$y = kt^n \quad (4)$$

$$\ln y = \ln k + n \ln t \quad (5)$$

where y is the thickness of interfacial IMC at t time, k is the grow rate constant, n is time index.

Figure 7 shows relationship between the average interfacial Cu_6Sn_5 IMC layer thickness and bonding time. The interfacial Cu_6Sn_5 layer from cold end and hot end presents distinct growth behavior, as is shown in Fig. 7a. The thickness of Cu_6Sn_5 layer from cold end shows a linear relationship with bonding time, however, the thickness of interfacial Cu_6Sn_5 layer from hot end grows slowly, which results in different growth rate of Cu_6Sn_5 in cold end and hot end during temperature gradient. The thickness of Cu_6Sn_5 layer shows a linear relationship with bonding time in $\ln-\ln$ format, as is shown in Fig. 7b. Each growth mechanism is related with the value of n . When $n = 1$, the IMC growth is controlled by interfacial reaction. When $n = 0.5$, the IMC growth is controlled by bulk diffusion. When $n = 0.33$, the IMC growth is controlled by grain boundary diffusion. The n for cold end is 0.97, which indicates that the Cu_6Sn_5 layer growth is controlled by interfacial reaction. The n for hot end is 0.18, indicating the growth of Cu_6Sn_5 hardly grows. The n for

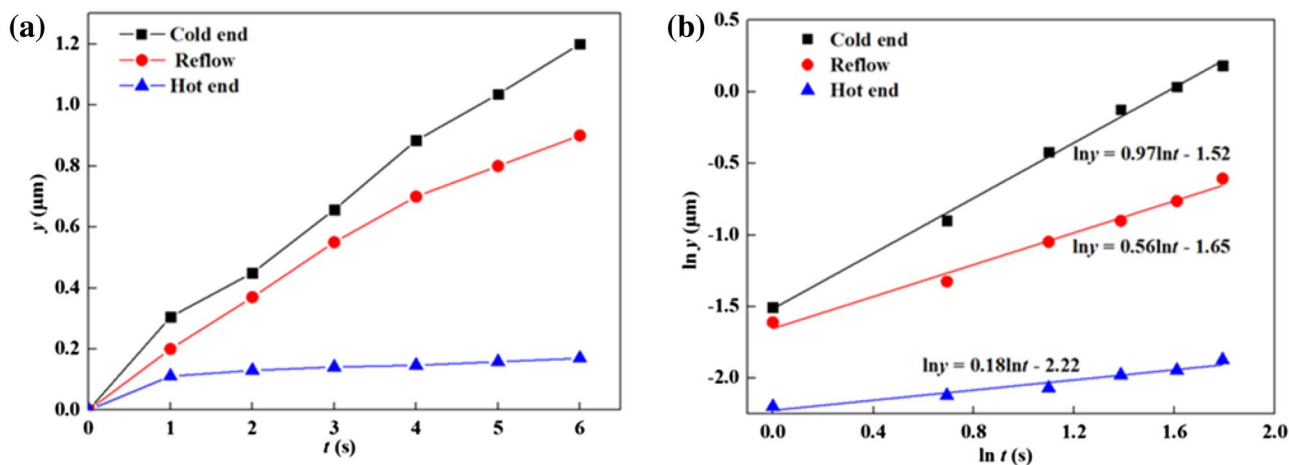


Fig. 7 The relationship between the thickness of interfacial Cu_6Sn_5 layer and the bonding time: a $y-t$; b $\ln y-\ln t$

Table 1 The values of average growth rate and time index

	Average growth rate ($\mu\text{m/s}$)	Time index n
Cold end	2.8×10^{-2}	0.18
Reflow	1.5×10^{-1}	0.56
Hot end	2.0×10^{-1}	0.97

reflow is 0.56, which indicates that the growth of interfacial Cu_6Sn_5 is controlled by volume diffusion. It is noted that the growth rate of interfacial Cu_6Sn_5 layer during temperature gradient is much higher than that of reflow. The values of average growth rate and time index under different reaction conditions are listed in Table 1. From Table 1, it can be seen that the average growth rate in reflowing is between cold end and hot end. It indicates that the temperature gradient dominates the IMC growth rate during bonding process, whereas reflowing temperature contributes little. The driving force of IMC formation is the difference in chemical potential between the two phases. When the flux of atoms runs into the IMC is larger than the flux of atoms runs off the IMC, the interfacial IMC layer grows. During temperature gradient, the flow of Cu atoms is only considered and the flow of Sn atoms is neglected, because Cu is the main diffuse atom for the interfacial reaction in Cu/Sn system.

From Fig. 7, it can be seen that the interfacial Cu_6Sn_5 layer grows symmetrically during the reflow process, the interfacial Cu_6Sn_5 layer shows asymmetric growth during thermal compression bonding process. It is well known that the growth rate of interfacial IMC layer at high temperature is faster than the growth rate of interfacial IMC layer at low temperature. However, the growth rate of Cu_6Sn_5 layer from cold end is obviously faster than the growth rate of Cu_6Sn_5 layer from hot end during thermal compression bonding process. Moreover, the average thickness of the interfacial

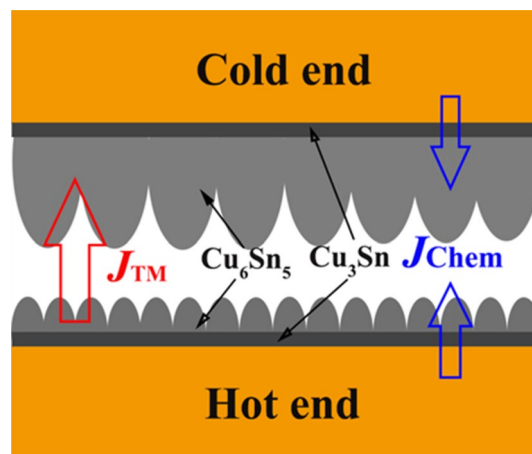


Fig. 8 The schematic of Cu atom flux in Cu/Sn/Cu system

Cu_6Sn_5 layer during reflow process is between the hot end and cold end of the interfacial Cu_6Sn_5 layer during temperature gradient, which means that the flux of Cu atoms from hot end migrates to cold end across the liquid Sn layer during temperature gradient.

3.4 The analysis of interfacial IMC formation mechanism

In order to reveal the effect mechanism of temperature gradient, the asymmetric growth of Cu_6Sn_5 leads to the source of Cu atoms from cold end and hot end also being asymmetric. In other words, the amount of Cu atoms from hot end is significantly bigger than that from cold end. Figure 8 shows the schematic of temperature gradient bonding mechanism. Cu atoms from the Cu substrate and Cu atoms in the Cu_6Sn_5 layer at hot end are dissolved into the liquid Sn. The

dissolution of Cu atoms migrates from hot end to cold end introduced by temperature gradient [26]. The dissolution process makes Cu_6Sn_5 layer from hot end thinner than that of Cu_6Sn_5 layer from cold end. When Cu atoms reach the cold end, it contributes to form scallop-like Cu_6Sn_5 layer. Because of the formation rate of Cu_6Sn_5 is very fast during cooling, which will lead to the decrease of interfacial Cu concentration, especially in cold end [27]. Therefore, the Cu concentration near the cold end after solidification is lower than the Cu concentration of the solder layer. A similar phenomenon also occur during the aging process when the concentration distribution dominated by thermal migration [28, 29]. Moreover, the steady state solute concentration gradient is related with the temperature gradient, which can be expressed as [30]:

$$\frac{d \ln C}{dx} = \frac{-Q^*}{kT^2} \frac{dT}{dx} \quad (6)$$

where C is the concentration of Cu, Q^* is the heat of transport, k is Boltzmann constant, dT/dx is temperature, T is the bonding temperature. With the Cu atoms continue migrate from hot end to cold end, Q^* is positive value. According to Eq. (6), the concentration gradient of Cu atoms is contrast to the temperature gradient, which means the Cu concentration from cold end is higher than that of hot end. Therefore, the large amount of Cu–Sn clusters contributes to the rapid growth of interfacial Cu_6Sn_5 layer from cold end [31], the growth of interfacial Cu_6Sn_5 from hot end is significantly restrained. Therefore, the fast growth of interfacial Cu_6Sn_5 layer from cold end is mainly caused by thermal migration. The Cu atoms in the liquid solder play a crucial role in the growth of interfacial Cu_6Sn_5 layer.

The combined effect of the chemical potential gradient flux and temperature gradient flux of Cu in liquid Sn at both sides can be expressed as:

$$J_{\text{Cu-cold}} = J_{\text{chem-Cu}} - J_{\text{TM-Cu}} \quad (7)$$

$$J_{\text{Cu-hot}} = J_{\text{chem-Cu}} + J_{\text{TM-Cu}} \quad (8)$$

where $J_{\text{Chem-Cu}}$ represents Cu atoms flux caused by chemical potential gradient, $J_{\text{TM-Cu}}$ represents Cu atoms flux by temperature gradient.

At cold end, $J_{\text{Chem-Cu}}$ and $J_{\text{TM-Cu}}$ are in opposite directions, which will result in limited consumption of Cu substrate, a small fraction of Cu atoms from Cu substrate will migrate to the liquid Sn solder. At hot end, $J_{\text{Chem-Cu}}$ and $J_{\text{TM-Cu}}$ are in same directions, which will accelerate the consumption of Cu substrate, the Cu atoms diffused into the liquid solder from Cu substrate are also significantly enhanced.

The Cu concentration at cold end is saturated or nearly saturated, however, the Cu concentration at hot end is in an unsaturated state. As a result, the growth of interfacial IMC at cold end promotes, the growth of interfacial IMC

at hot end inhibits. In fact, the formation and dissolution of the interfacial IMC layer occur simultaneously. According to Dybkov's model [32], the dissolution rate of IMC in liquid Sn can be expressed as:

$$\frac{dC}{dt} = K_d \frac{S}{V} (C_s - C) \quad (9)$$

where C_s is the solute solubility in the solder, K_d is the dissolution rate constant, S is the contact area between the solid and the liquid solder, and V is the volume of the solder. According to the Eq. (9), the dissolution rate of interfacial IMC is proportional to $(C_s - C)$. Therefore, the lower the $(C_s - C)$ is, the slower the interfacial IMC dissolves. The formation of interfacial IMC is due to the local solute concentration approaching C_s . Due to the saturated or near saturated Cu concentration at cold end, the growth of interfacial IMC dominates. Meanwhile, the Cu atom dissolved from hot end continues to diffuse outward during temperature gradient, resulting in a local Cu concentration lower than C_s , which keeps the newly formed interfacial IMC from hot end balance in the solder. At this stage, the flux caused by thermal migration is the largest contributor to the depletion of Cu substrates from hot end. The Cu atom from hot end dissolves more obviously under the thermal migration, therefore, the growth of interfacial IMC from cold end exhibits abnormally fast.

4 Conclusion

A new TLP bonding process (temperature gradient bonding) is proposed in this paper. Compared to conventional homogeneous bonding temperature, a temperature gradient is superimposed across the liquid solder during temperature gradient bonding. The results show that temperature gradient contributes to the mass migration of Cu atoms from hot end to cold end. The scallop-like Cu_6Sn_5 and planar-like Cu_3Sn are formed between solid Cu and liquid Sn at initial stage. The growth rate of Cu_6Sn_5 layer at cold end is faster than that of hot end, this is due to the fact that the Cu atoms migrate from hot end to cold end by temperature gradient. The liquid Sn layer thickness decreases with increasing bonding time. The Cu_6Sn_5 and Cu_3Sn are consisted of the solder joints after the liquid Sn layer is completely consumed. The morphology of Cu_3Sn grows from planar-like morphology to scallop-like morphology with increasing bonding time. The final solder joint is consisted of Cu_3Sn . The formation time of full IMCs solder joints can be narrowed by temperature gradient, which offers a new method for fabricating interconnect material rapidly and efficiently for the next generation semiconductor power devices.

Acknowledgements This work is supported by the National Natural Science Foundation of China (51174069) and National High Technology Research and Development Program (863 Program) of China (No. 2015AA033304).

References

- R. Kisiel, Z. Szczepeński, Die-attachment solutions for SiC power devices. *Microelectron. Reliab.* **49**(6), 627–629 (2009)
- P.G. Neudeck, R.S. Okojie, L.Y. Chen, High-temperature electronics—a role for wide bandgap semiconductors? *Proc. IEEE* **90**(6), 1065–1076 (2002)
- D.G. Senesky, Wide bandgap semiconductors for sensing within extreme harsh environments. *ECS Trans.* **50**(6), 233–238 (2013)
- J. Glazer, Microstructure and mechanical properties of Pb-free solder alloys for low-cost electronic assembly: a review. *J. Electron. Mater.* **23**(8), 693–700 (1994)
- R.W. Wu, L.C. Tsao, R.S. Chen, Effect of 0.5 wt% nano-TiO₂ addition into low-Ag Sn0.3Ag0.7Cu solder on the intermetallic growth with Cu substrate during isothermal aging. *J. Mater. Sci. Mater. Electron.* **26**(3), 1858–1865 (2015)
- Y. Li, K. Moon, C.P. Wong, Electronics without Lead. *Science* **308**(5727), 1419–1420 (2005)
- M. Abteu, G. Selvaduray, Lead-free solders in microelectronics. *Mater. Sci. Eng. R* **27**(5–6), 95–141 (2000)
- J.Y. Tsai, C.W. Chang, Y.C. Shieh, Y.C. Hu, C.R. Kao, Controlling the microstructure from the gold-tin reaction. *J. Electron. Mater.* **34**(2), 182–187 (2005)
- H.G. Song, J.P. Ahn, J.W. Morris, The microstructure of eutectic Au-Sn solder bumps on Cu/electroless Ni/Au. *J. Electron. Mater.* **30**(9), 1083–1087 (2001)
- L.M. Yin, D. Li, Z.X. Yao, G. Wang, A. Blackburn, Microstructures and properties of Bi-10Ag high temperature solder doped with Cu element. *Microelectron. Reliab.* **80**, 79–84 (2018)
- S. Kim, K.S. Kim, S.S. Kim, K. Sukanuma, Interfacial reaction and die attach properties of Zn-Sn high-temperature solders. *J. Electron. Mater.* **38**(2), 266–272 (2009)
- K. Sukanuma, S. Sakamoto, N. Kagami, D. Wakuda, K.S. Kim, M. Nogi, Low-temperature low-pressure die attach with hybrid silver particle paste. *Microelectron. Reliab.* **52**(2), 375–380 (2012)
- S.Y. Zhao, X. Li, Y.H. Mei, G.Q. Lu, Study on high temperature bonding reliability of sintered nano-silver joint on bare copper plate. *Microelectron. Reliab.* **55**(12), 2524–2531 (2015)
- S.A. Paknejad, A. Mansourian, J. Greenberg, K. Khtatba, L.V. Parijs, S.H. Mannan, Microstructural evolution of sintered silver at elevated temperatures. *Microelectron. Reliab.* **63**, 125–133 (2016)
- S.A. Paknejad, S.H. Mannan, Review of silver nanoparticle based die attach materials for high power/temperature applications. *Microelectron. Reliab.* **70**, 1–11 (2017)
- Y. Zhou, W.F. Gale, T.H. North, Modelling of transient liquid phase bonding. *Int. Mater. Rev.* **40**(5), 181–196 (1995)
- W.F. Gale, D.A. Butts, Transient liquid phase bonding. *Sci. Technol. Weld. Join.* **9**(4), 283–300 (2004)
- H.A. Mustain, W.D. Brown, S.S. Ang, Transient liquid phase die attach for high-temperature silicon carbide power devices. *IEEE Trans. Compon. Packag. Technol.* **33**(3), 563–570 (2010)
- M. Fujino, H. Narusawa, Y. Kuramochi, E. Higurashi, T. Suga, T. Shiratori, M. Mizukoshi, Transient liquid-phase sintering using silver and tin powder mixture for die bonding. *Jpn. J. Appl. Phys.* **55**(4S), 04EC14 (2016)
- N.S. Bosco, F.W. Zok, Strength of joints produced by transient liquid phase bonding in the Cu-Sn system. *Acta Mater.* **53**(7), 2019–2027 (2005)
- B.L. Liu, Y.H. Tian, C.X. Wang, R. An, Y. Liu, Extremely fast formation of Cu-Sn intermetallic compounds in Cu/Sn/Cu system via a micro-resistance spot welding process. *J. Alloys Compd.* **687**, 667–673 (2016)
- Z.Z. Yin, F.L. Sun, M.J. Guo, The fast formation of Cu-Sn intermetallic compound in Cu/Sn/Cu system by induction heating process. *Mater. Lett.* **215**, 207–210 (2017)
- H.J. Ji, M.G. Li, S. Ma, M.Y. Li, Ni₃Sn₄-composed die bonded interface rapidly formed by ultrasonic-assisted soldering of Sn/Ni solder paste for high-temperature power device packaging. *Mater. Des.* **108**, 590–596 (2016)
- J.W. Yoon, J.G. Lee, J.B. Lee, B.I. Noh, S.B. Jung, Thermo-compression bonding of electrodes between FPCB and RPCB by using Pb-free solders. *J. Mater. Sci. Mater. Electron.* **23**(1), 41–47 (2012)
- H.Y. Chen, C. Chen, Thermomigration of Cu-Sn and Ni-Sn intermetallic compounds during electromigration in Pb-free SnAg solder joints. *J. Mater. Res.* **26**(8), 983–991 (2011)
- C. Chen, H.Y. Hsiao, Y.W. Chang, F.Y. Ouyang, K.N. Tu, Thermomigration in solder joints. *Mater. Sci. Eng. R* **73**(9), 85–100 (2012)
- L. Qu, N. Zhao, H.T. Ma, H.J. Zhao, M.L. Huang, In situ study on the effect of thermomigration on intermetallic compounds growth in liquid-solid interfacial reaction. *J. Appl. Phys.* **115**(20), 204907 (2014)
- F.Y. Ouyang, C.L. Kao, In situ observation of thermomigration of Sn atoms to the hot end of 96.5Sn-3Ag-0.5Cu flip chip solder joints. *J. Appl. Phys.* **110**(12), 123525 (2011)
- F.Y. Ouyang, K.N. Tu, Y.S. Lai, A.M. Gusak, Effect of entropy production on microstructure change in eutectic SnPb flip chip solder joints by thermomigration. *Appl. Phys. Lett.* **89**(22), 221906 (2006)
- P. Shewmon, *Diffusion in Solids* (Springer, Switzerland, 2016)
- N. Zhao, X.M. Pan, D.Q. Yu, H.T. Ma, L. Wang, Viscosity and surface tension of liquid Sn-Cu lead-free solders. *J. Electron. Mater.* **38**(6), 828–833 (2009)
- V.I. Dybkov, *Growth Kinetics of Chemical Compound Layers* (International Science Publishing, Cambridge, 1998)